Antimicrobial Agents and Chemotherapy

Low-Molecular-Mass Penicillin Binding Protein 6b (DacD) Is Required for Efficient GOB-18 Metallo-β-Lactamase Biogenesis in Salmonella enterica and Escherichia coli

Luciano Brambilla, Jorgelina Morán-Barrio and Alejandro M. Viale

Antimicrob. Agents Chemother. **2014, 58(1):205. DOI: 10.1128/AAC.01224-13.**
Published Ahead of Print 21 October 2013.

AAC
Journals.ASM.org

Low-Molecular-Mass Penicillin Binding Protein 6b (DacD) Is Required for Efficient GOB-18 Metallo-β-Lactamase Biogenesis in *Salmonella enterica* and *Escherichia coli*

Luciano Brambilla, Jorgelina Morán-Barrio, Alejandro M. Viale

Departamento de Microbiología and Instituto de Biología Molecular y Celular de Rosario (IBR, CONICET-UNR), Facultad de Ciencias Bioquímicas y Farmacéuticas, Universidad Nacional de Rosario, Rosario, Argentina

Metallo-β-lactamases (MBLs) are Zn^{2+}-containing secretory enzymes of clinical relevance, whose final folding and metal ion assembly steps in Gram-negative bacteria occur after secretion of the apo form to the periplasmic space. In the search of periplasmic factors assisting MBL biogenesis, we found that *dacD* null (Δ*dacD*) mutants of *Salmonella enterica* and *Escherichia coli* expressing the pre-GOB-18 MBL gene from plasmids showed significantly reduced resistance to cefotaxime and concomitant lower accumulation of GOB-18 in the periplasm. This reduced accumulation of GOB-18 resulted from increased accessibility to proteolytic attack in the periplasm, suggesting that the lack of DacD negatively affects the stability of secreted apo MBL forms. Moreover, Δ*dacD* mutants of *S. enterica* and *E. coli* showed an altered ability to develop biofilm growth. DacD is a widely distributed low-molecular-mass (LMM) penicillin binding protein (PBP6b) endowed with low DD-carboxypeptidase activity whose functions are still obscure. Our results indicate roles for DacD in assisting biogenesis of particular secretory macromolecules in Gram-negative bacteria and represent to our knowledge the first reported phenotypes for bacterial mutants lacking this LMM PBP.

β-Lactamase production represents a common mechanism of bacterial resistance and cause of failure in the treatment of infections (1). Among the different groups of β-lactamases defined on the basis of structural similarity and catalytic mechanisms, the metallo-β-lactamases (MBLs) are especially worrisome (2, 3). This group is constituted entirely of metalloenzymes employing Zn^{2+} for catalysis; members of this group can hydrolyze a broad spectrum of substrates, including the latest generations of clinically relevant β-lactams, and can be rapidly spread by horizontal gene transfer (1–3). Among the different strategies for controlling MBL dissemination, efforts have so far been focused on the design of a general MBL inhibitor, a goal so far hindered by the diversity of active-site structures among these metalloenzymes (4).

A less known aspect of MBL research, but one that may provide potential targets for antimicrobial drug design, is the MBL biogenesis pathway (5). We previously reported that the productive biogenesis of the GOB-18 MBL in *Escherichia coli* requires an "expanded" DnaK chaperone system to assist the cytoplasmic transit of the preapoprotein to the secretion system (5). Moreover, we also found that secretion of the apo GOB-18 form is driven by the Sec (SecA-SecYEG) machinery, implying that final folding and Zn^{2+} ion assembly to the native MBL conformation occur in the periplasm (5). Unfolded proteins emerging from the Sec channel are greeted by a highly complex macromolecule-crowded environment containing an array of modifying enzymes, some of them endowed with the ability to act as folding assistants (6–8). This complex scenario can certainly affect individual folding landscapes (6), but whether the final steps of MBL folding and Zn^{2+} assembly are assisted by periplasmic factors is yet obscure (5). Yet, different lines of evidence suggest that this might be the case. First, *in vitro* assays have shown that Zn^{2+} binding (and therefore final folding) by different apo MBL forms requires β-lactam substrates, suggesting that ion-less nonnative forms might prevail *in vivo* in their absence (9). Due to the high protease content of the periplasm, some means of protection of these nonnative forms from degradation must exist (10), thus suggesting the existence of periplasmic factors performing this role, which is typical of folding assistants (8). Second, production of different apo MBL forms in the *E. coli* cytoplasm by means of expression vectors lacking transit sequences directing secretion resulted in the accumulation in this compartment of mostly Fe-containing inactive MBLs (11, 12). By contrast, Zn-containing native MBLs are predominantly recovered when the same apoproteins are directed to the periplasm (11, 12), suggesting the existence of factors in this compartment mediating Zn^{2+} supply or assisting folding (or refolding) until the native conformation is reached.

By using different genetic approaches we searched here for the existence of factors assisting biogenesis of the GOB-18 MBL in the periplasm of *Escherichia coli* and *Salmonella enterica*. For this purpose the preapoprotein was produced from expression plasmids (5) and the resulting GOB-18-mediated cefotaxime (CTX) resistance of the cells was analyzed. *E. coli* mutants lacking periplasmic proteins with chaperone capabilities, including SurA, FkpA, DegP, PpiA, PpiD, DsbA, DsbC, and DsbG (6, 7), showed no significant reductions in GOB-mediated CTX resistance. Yet a different approach using *S. enterica* MudJ transposon mutagenesis showed that an insertion in the *phsABC-dacD* cluster (13, 14) was associated with reduced GOB-18-mediated CTX resistance. This phenotype could be associated with the deletion of the *dacD* gene in *S. enterica* and also in *E. coli*, concomitant with a lower accumulation of GOB-18 in the periplasm of the Δ*dacD* mutants. *dacD*

Received 7 June 2013 Returned for modification 26 June 2013
Accepted 14 October 2013
Published ahead of print 21 October 2013
Address correspondence to Alejandro M. Viale, viale@ibr-conicet.gov.ar.

doi:10.1128/AAC.01224-13

TABLE 1 Bacterial strains and plasmids used in this work

Strain or plasmid	Characteristics	Source or reference
Strains		
S. enterica		
1344	Laboratory strain, *hisG* autotroph	28
14028	Laboratory strain	ATCC
1344 RCR	*S. enterica* 1344 *phsB*::miniMudJ::*npt* (Km^r) bearing p-preGOB	This work
14028 RCR	*S. enterica* 14028 *phsB*::miniMudJ::*npt* (Km^r) bearing p-preGOB	This work
1344 Δ*dacD*	*S. enterica* 1344 Δ*dacD*::*npt* (Km^r), generated by replacing the *dacD* gene with an *npt* cassette	This work
E. coli		
DH5α	*fhuA2* Δ(*argF-lacZ*)*U169 phoA glnV44* ϕ80d*lacZ*ΔM15 *gyrA96 recA1 relA1 endA1 thi-1 hsdR17*	37
BW25113	Δ(*araD-araB*)*567* Δ*lacZ4787*::*rrnB-3* λ^- *rph-1* Δ(*rhaD-rhaB*)*568 hsdR514*	21
BW25113 Δ*dacD*	Δ*dacD*::*npt* (Km^r)	21
BW25113 Δ*dacD**	BW25113Δ*dacD* in which the *npt* cassette was removed; Km sensitive	This work
BW25113 Δ*fkpA*	Δ*fkpA*::*npt* (Km^r)	21
BW25113 Δ*ppiD*	Δ*ppiD*::*npt* (Km^r)	21
BW25113 Δ*ppiA*	Δ*ppiA*::*npt* (Km^r)	21
BW25113 Δ*dsbG*	Δ*dsbG*::*npt* (Km^r)	21
BW25113 Δ*dsbA*	Δ*dsbA*::*npt* (Km^r)	21
BW25113 Δ*dsbB*	Δ*dsbB*::*npt* (Km^r)	21
BW25113 Δ*degP*	Δ*degP*::*npt* (Km^r)	21
Plasmids		
p-preGOB	pACYC184 derivative, directs expression of *pre-apo-gob-18* gene cloned from *Elizabethkingia meningoseptica* under *araBAD* promoter control (Cm^r)	5
pBluescript SK(−)	Cloning vector, pBR322 derivative (Amp^r)	37
p-PHS	pBluescript derivative containing *phsABC* from *S. enterica* cloned into BamHI and EcoRI sites (Amp^r)	This work
pKD20	Red recombinase expression plasmid (Amp^r)	23
pBAD18	Expression vector; contains *araBAD* promoter (Km^r)	24
pBDacD	pBAD-18 derivative; expression plasmid for the cloned *E. coli dacD* gene under *araBAD* promoter control (Km^r)	This work

encodes the low-molecular-mass (LMM) penicillin binding protein 6b (PBP6b), ubiquitously present in Gram-negative bacteria but of still poorly defined function(s) (15–20). Moreover, the Δ*dacD* mutants of both species showed altered biofilm growth. Our results indicate roles for DacD in the biogenesis of particular secretory macromolecules in Gram-negative bacteria and provide the first reported bacterial phenotypes associated with the loss of this LMM PBP.

MATERIALS AND METHODS

Bacterial strains and plasmids. *S. enterica* and *E. coli* laboratory strains and plasmids used in this work are listed in Table 1. The *E. coli* K-12 strain BW25113 wild type (wt) and derived mutants were obtained from the Keio collection (21).

Culture conditions and induction and analysis of GOB-18 production. All bacterial strains were grown aerobically at 37°C in LB medium supplemented with the appropriate antibiotics where required (kanamycin [Km], 25 μg/ml; chloramphenicol [Cm], 15 μg/ml; ampicillin, 100 μg/ml). For pre-apo GOB-18 production in bacteria transformed with plasmid p-preGOB, the cells were grown in LB liquid medium in the presence of 15 μg/ml Cm to an absorbance at 660 nm (A_{660}) of 0.3 and L-arabinose was added at this step to a final concentration of 0.2% (wt/vol). Incubation was continued under these conditions, and cell aliquots were removed at the times indicated in the figures for the analysis of GOB-18 in periplasmic fractions by SDS-PAGE and immunoblotting as described previously (5).

Evaluation of bacterial CTX resistance phenotypes. The different *S. enterica* and *E. coli* strains and derived mutants bearing p-preGOB were grown aerobically at 37°C in Cm-containing LB liquid medium to an A_{660} of 0.3 as above. Aliquots were withdrawn and sequentially diluted 10-fold, and 5 μl of each of these dilutions was poured on the surface of LB agar plates containing 0.2% (wt/vol) L-arabinose, 15 μg/ml Cm, and 0.1 μg/ml CTX. A replica plate lacking CTX was used to evaluate differences in growth behavior due to the particular mutations analyzed. Differences in GOB-mediated CTX resistance were evaluated after incubation at 37°C for 24 h.

CTX MIC values were estimated by the agar dilution technique as previously described (5). In short, the analyzed bacterial strains were grown as above and induced with L-arabinose. After an additional 1 h of incubation under these conditions, culture aliquots were adjusted to an A_{660} of 0.3 with fresh LB medium and sequentially diluted 10-fold, and 5 μl of each dilution was poured onto the surface of LB agar plates supplemented with CTX at concentrations ranging from 0.01 to 25 μg/ml. MIC values were estimated after 24 h at 37°C.

***S. enterica* MudJ mutagenesis and screening.** A library was constructed on *S. enterica* 1344 cells harboring plasmid p-preGOB by MudJ transposon mutagenesis (22), and mutants were analyzed for reduced CTX resistance by replica plating in the absence or presence of 0.1 μg/ml CTX on Km- and Cm-LB agar plates supplemented with 0.2% (wt/vol) L-arabinose. From 5 clones out of 11,336 colonies analyzed initially displaying this phenotype, one consistently regenerated P22-mediated transductants in fresh *S. enterica*/p-preGOB backgrounds, maintaining the reduced CTX-resistant phenotype. These transductants were designated RCR (for reduced CTX resistance) and used for further analyses. These cells were also used to further transduce the MudJ mutated locus to fresh *S. enterica* backgrounds lacking p-preGOB (see Table 2 and Fig. 4).

Southern hybridization using a ^{32}P-labeled *npt* probe indicated a single MudJ chromosomal insertion in RCR cells (not shown). Chromosomal DNA was isolated from these cells, digested with EcoRI and BamHI, ligated to plasmid pBluescript SK(−), and transformed into competent *E. coli* DH5α cells. After selection in LB agar plates containing 25 μg/ml Km and 100 μg/ml ampicillin, plasmids were isolated from different colonies and used to identify by sequence analysis the *S. enterica* chromosomal locus targeted by MudJ.

Construction of a plasmid directing expression of *S. enterica phsABC* genes. A PCR fragment encompassing the *S. enterica phsABC* DNA region from 67 bp upstream of the *phsA* initiation codon (including promoter sequences) to 17 bp downstream of *phsC* (see Fig. 1D) was generated by using purified DNA from *S. enterica* 1344 cells and *phs* forward (5′-CTCggatccT TGAAGCCGACATTTC-3′) and reverse (5′-CACgaattcATTATTTTATG GATACGC-3′) primers designed from published sequence data (14). BamHI and EcoRI sites (lowercase letters) were additionally incorporated into the forward and reverse primers, respectively, for subsequent cloning purposes. The PCR product was digested with BamHI and EcoRI, ligated into pBluescript SK(−) (Table 1), and transformed into competent *E. coli* DH5α cells as above. The cells were plated on LB agar containing 100 μg/ml ampicillin and incubated for 48 h at 37°C, and different colonies were tested for the newly acquired cell ability to produce H_2S from thiosulfate (14). A plasmid isolated from an H_2S-producing *E. coli* clone was found by restriction mapping to bear the *S. enterica phsABC* genes (14) and was designated p-PHS (Table 1) for further studies.

Construction of *S. enterica* Δ*dacD* mutants. The *dacD* gene of *S. enterica* 1344 was replaced by an *npt* cassette by following previously described procedures (23). In short, a DNA fragment containing the *npt* gene and *S. enterica dacD* neighboring regions was generated by PCR

using primers dacD-direct (5′-ACTGAACTTCCGTAAAAAGAACGGC AAATAGAGACCATCCTGAGGACATGATTCCGGGGATCCGTCGAC C-3′) and dacD-reverse (5′-TGACGGTGAACGGTGTGTGTGACAACG GCTTACGCTTTATGCTGAAAATATGTAGGCTGGAGCTGCTTCG-3′), designed after the *npt* cassette (23) and the *S. enterica dacD* neighboring regions (GenBank accession number AE014613.1). After transformation into *S. enterica* 1344 cells bearing plasmid pKD20 (23), Δ*dacD*::*npt* cells were selected in LB agar plates containing 50 μg/ml Km, and the replacement was confirmed in several clones by PCR. A selected clone was used to grow P22 phage to further transduce the Δ*dacD*::*npt* allele to fresh *S. enterica* backgrounds (Table 1).

Complementation of *E. coli* Δ*dacD* mutants with a plasmid directing controlled expression of the *dacD* gene. The *E. coli dacD* gene was amplified by PCR and cloned in a pBAD derivative conferring Km resistance (24) using the same primers and procedures described by other authors (19). After the appropriate construction was confirmed by sequence analysis, the *dacD* expression plasmid (pBDacD) (Table 1) was transformed into *E. coli* BW25113 Δ*dacD* mutants from which the *npt* cassette had been previously removed (21) (*E. coli* Δ*dacD** mutants) (Table 1). These cells were subsequently transformed with plasmid p-preGOB (Table 1), and the effects of restoring *dacD* in *trans* on GOB-mediated cell CTX resistance were assayed. Parallel controls were also conducted using *E. coli* Δ*dacD**/p-preGOB cells transformed with the empty pBAD-Km vector. Since uncontrolled expression of *dacD* from plasmids may be deleterious and even promote cell lysis (16), different L-arabinose inducer concentrations were tested in experiments using pBDacD. We found that 0.002% (wt/vol) L-arabinose represented the optimal compromise between obtaining maximal GOB-18 induction while simultaneously preventing significant cell lysis.

Cell fractionation procedures and analysis by SDS-PAGE. Periplasmic fractions were isolated by subjecting *S. enterica* or *E. coli* cells to hypo-osmotic shock by following previously described protocols (25). Possible cross-contaminations with cytoplasmic proteins were assayed by analyzing GroEL and DnaK contents in these fractions by immunoblotting in accordance with previously described procedures (5). Total cell extracts (5) and outer membrane (OM) fractions (26) were isolated by following previously described procedures. The protein profiles of these fractions were obtained by SDS-PAGE using 12% (wt/vol) polyacrylamide gels. Immunoblot analysis using anti-GOB-18, anti-GroEL, anti-DnaK, anti-OmpA, or anti-OmpW was conducted by following previously described procedures (5).

Functional evaluation of OM integrity. We essentially followed previously described procedures to evaluate the SDS cell sensitivity of *S. enterica* RCR mutants (27).

Biofilm formation. Biofilm growth was studied by analyzing bacterial adherence to polystyrene surfaces (28) and colony morphotype on Congo red agar plates (29).

Other. DNA sequencing was conducted at the DNA Sequencing Service of Maine University (Orono, ME).

RESULTS

GOB-18-mediated CTX resistance in *E. coli* strains with mutations in genes encoding periplasmic chaperones. Different experimental data indicate that a number of periplasmic proteins displaying peptidyl-prolyl isomerase (SurA, FkpA, PpiD, PpiA), disulfide isomerase (DsbA, DsbC, DsbG), or protease (DegP) activities are also endowed with ability to assist in the folding of a number of *E. coli* envelope proteins (6, 7). We thus evaluated first whether any of them could also assist GOB-18 folding by analyzing the CTX resistance phenotypes of the corresponding *E. coli* mutants (Table 1) bearing p-preGOB. None of these mutations, however, promoted significant reductions in the CTX resistance, as judged by the MIC values of the corresponding cells, which were similar or identical to that of the wt strain containing p-preGOB (data not shown).

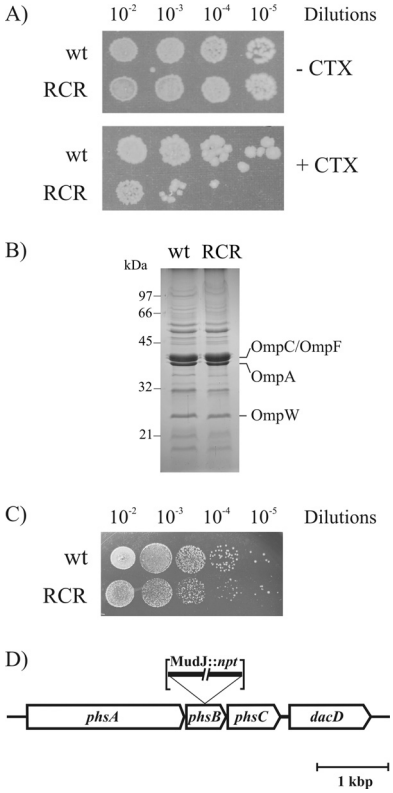

FIG 1 Characterization of *S. enterica* RCR mutants. (A) RCR cells display reduced GOB-18-mediated CTX resistance. Growth of 10-fold-diluted cultures of *S. enterica* 1344 RCR mutants (RCR) and the corresponding wt cells bearing plasmid p-preGOB in the absence (−CTX) or presence of 0.1 μg/ml CTX (+CTX) is shown. (B) OM protein profiles of the above *S. enterica* strains analyzed by SDS-PAGE. The identity and final positions of characteristic OM proteins are indicated on the right. (C) SDS sensitivity assay of the above *S. enterica* strains. (D) *S enterica* 1344 chromosomal locus targeted by the MudJ transposon. For details see Materials and Methods.

This suggests no significant individual roles for the corresponding periplasmic proteins in GOB-18 biogenesis.

Isolation of *S. enterica* RCR mutants displaying reduced GOB-mediated CTX resistance. We next constructed a library of MudJ insertional mutants on *S. enterica* 1344 cells bearing p-preGOB and searched for clones displaying reductions in CTX resistance (see Materials and Methods for details). One initially identified mutant clone consistently regenerated transductants displaying reduced CTX resistance in *S. enterica* 1344 and 14028 genetic backgrounds (Fig. 1A and Table 2). These transductant lineages were designated RCR (for reduced CTX resistance) and used for further phenotypic and genotypic characterization.

No differences in *S. enterica* RCR growth rates compared to those of their isogenic (p-preGOB-containing) wt strains were observed in Cm-containing LB liquid medium in the absence of CTX (not shown), indicating no growth defects due to the MudJ insertion in these mutants.

RCR mutants showed no significant alterations in OM composition or SDS permeability. We evaluated next whether the chromosomal disruption generated by the MudJ insertion could alter RCR OM functions. However, neither a significant change in OM protein profiles (Fig. 1B) nor increased susceptibility to SDS (Fig. 1C) could be observed in RCR mutants compared to wt cells

TABLE 2 Intrinsic and GOB-mediated CTX resistance phenotypes of the *S. enterica* and *E. coli* strains and mutants analyzed in this work[a]

Bacterial strain	MIC for CTX (μg/ml)
S. enterica	
1344	0.07
1344 *phsB*::MudJ	0.07
1344 Δ*dacD*	0.07
1344/p-preGOB	10
1344 RCR (*phsB*::MudJ/p-preGOB)	7.5
1344 Δ*dacD*/p-preGOB	7.5
14028	0.08
14028 *phsB*::MudJ	0.08
14028 Δ*dacD*	0.08
14028/p-preGOB	20
14028 RCR (*phsB*::MudJ/p-preGOB)	9
14028 Δ*dacD*/p-preGOB	9
14028 RCR/pBS	6
14028 RCR/p-PHS	6
E. coli	
BW25113	0.05
BW25113 Δ*dacD*::*npt*	0.05
BW25113 Δ*dacD**	0.05
BW25113/p-preGOB	9
BW25113 Δ*dacD*::*npt*/p-preGOB	2
BW25113 Δ*dacD**/pBAD18/p-preGOB	1
BW25113 Δ*dacD**/pBDacD/p-preGOB	4

[a] The different *S. enterica* and *E. coli* strains and derived mutants, as well as the plasmids employed, are detailed in Table 1. MICs for CTX were estimated as detailed in Materials and Methods.

bearing p-preGOB. These results indicated no substantial defects in OM composition or permeability in RCR cells. In line with these observations, the intrinsic CTX resistance of mutants bearing the MudJ insertion but lacking plasmid p-preGOB (Table 1) was similar or identical to that of the corresponding isogenic wt strains (Table 2).

MudJ is inserted at the *phsABC-dacD* locus in *S. enterica* RCR cells. The chromosomal region targeted by MudJ in RCR cells was identified by cloning an EcoRI/HindIII chromosomal fragment containing a transposon fragment bearing the *npt* gene and adjacent regions (see Materials and Methods for details). Sequencing analyses revealed that MudJ was inserted into the *phsB* gene of the *S. enterica phsABC-dacD* genetic cluster (Fig. 1D), genes that are apparently cotranscribed (13, 14). *phsABC* genes encode the subunits of a periplasmic thiosulfate reductase involved in the dissimilatory reduction of thiosulfate to H_2S, a pathway common to *Salmonella* species but rarely present among other *Enterobacteriaceae* members (13, 14). *dacD* codes in turn for the LMM PBP6b, ubiquitously present in members of the *Enterobacteriaceae* family (15–19).

Mutational loss of *dacD* in *S. enterica* resulted in reductions in GOB-mediated CTX resistance phenotypes. Either the insertional inactivation of *phsB* or reductions in the expression of downstream genes could account for the reduced CTX resistance phenotypes of RCR cells. To distinguish between these possibilities, we first analyzed whether introduction of plasmid p-PHS containing the cloned *phsABC* genes could revert the reduced CTX resistance phenotype of RCR cells. However, as seen in Table 2, no significant recoveries of CTX resistance could be observed in RCR mutants transformed with p-PHS.

We next constructed *S. enterica* Δ*dacD* deletion mutants and tested whether these cells displayed reduced CTX resistance phenotypes. As seen in Table 2 and as judged by the MIC values obtained, Δ*dacD* mutants on 1344 and 14028 backgrounds displayed reductions in GOB-mediated CTX resistance similar to those for the corresponding RCR cells. By contrast, the intrinsic CTX resistance shown by mutant cells lacking p-preGOB was not substantially altered (Table 2).

The overall observations thus strongly pointed to the loss of DacD as being responsible for the reductions in GOB-mediated CTX resistance.

***E. coli* Δ*dacD* mutants also show reductions in GOB-mediated CTX resistance.** *E. coli* contains a *dacD* homolog displaying 87% identity to that of *S. enterica* and also lacks *phsABC* genes (13–15). We thus evaluated next whether Δ*dacD* mutants of *E. coli* cells also displayed reductions in GOB-mediated CTX resistance (Table 2). As shown in the table, this was also the case, as judged by the significantly reduced MIC values obtained for mutants bearing p-preGOB. Also, and similar to results for *S. enterica*, the intrinsic CTX resistance of *E. coli* Δ*dacD* mutants lacking the plasmid was not significantly affected (Table 2). This lack of effect of the Δ*dacD* mutation on intrinsic *E. coli* sensitivity to β-lactams has been observed previously by other authors (19).

We next evaluated whether restoration of *dacD* expression from plasmids could revert the losses of GOB-mediated CTX resistance shown by *E. coli* Δ*dacD* mutants (Table 2). As seen in the table, controlled *dacD* expression in these mutants (Δ*dacD**/pBDacD/p-preGOB mutants) partially restored the losses in CTX resistance, as judged by the 4-fold increases in MIC values compared to those for the same cells bearing the plasmid vector (Δ*dacD**/ pBAD18/p-preGOB).

These overall results indicate relevant roles for DacD in GOB-18 biogenesis in both *S. enterica* and *E. coli*.

***S. enterica* and *E. coli* Δ*dacD* mutants show reduced periplasmic contents of GOB-18.** We analyzed next whether the reductions in GOB-18-mediated CTX resistance shown by Δ*dacD* cells could be attributed to less accumulation of this MBL in the periplasm of these mutants. A time course analysis of GOB-18 contents in periplasmic fractions of *S. enterica* and *E. coli* indicated significantly reduced accumulation of this MBL in the corresponding Δ*dacD* mutants compared to that in wt cells (Fig. 2A and B, respectively). However, as seen in the same figure, the bulk of periplasmic proteins showed no significant changes between Δ*dacD* mutants and the corresponding wt cells, as judged by SDS-PAGE analyses (Fig. 2). A similar observation was made for the whole-cell protein profiles of Δ*dacD* mutants bearing p-preGOB, which showed no significant modifications compared to those of wt cells (Fig. 2C). It is worth noting that comparisons of the protein profiles shown in Fig. 2B and C indicated no appreciable contamination of periplasmic fractions with cytoplasmic contents in either Δ*dacD* mutants or wt cells, a result that also ruled out significant cell lysis due to the mutation. These conclusions are also supported by the very low to negligible levels of GroEL and DnaK cytoplasmic chaperones found in periplasmic fractions of both Δ*dacD* mutants and wt cells, as judged by immunoblot analyses (Fig. 2C).

The overall observations thus supported the notion that the absence of DacD affected in particular the last biogenesis steps of GOB-18 in the periplasm and that this, rather than general defects in

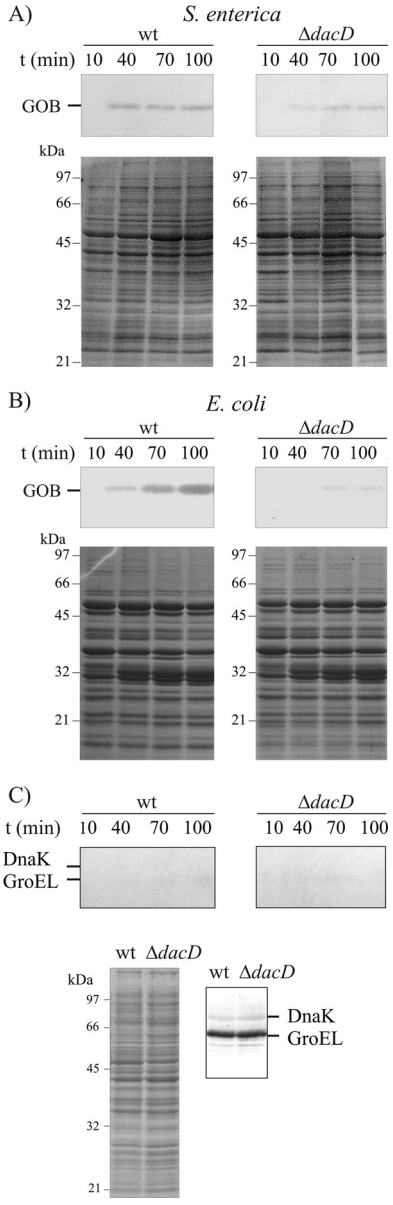

FIG 2 DacD mutational losses promote GOB-18 reductions in the periplasm. (A) Time course analysis of GOB-18 accumulation in periplasmic fractions of p-preGOB-containing wt *S. enterica* 1344 and isogenic Δ*dacD* mutants. (B) Time course accumulation of GOB-18 in periplasmic fractions of p-preGOB-containing wt *E. coli* BW25113 and isogenic Δ*dacD* mutants. In both cases the cells were grown at 37°C in LB liquid medium containing 15 μg/ml Cm to an A_{660} of 0.3 and L-arabinose (0.2% final) was added to induce GOB-18 production. Incubation was continued as above, and cell aliquots were taken at the indicated times to isolate the corresponding periplasmic fractions. In each case the lower part shows the SDS-PAGE profiles obtained from equivalent amounts of cells and the upper part shows the corresponding immunoblot analysis obtained with anti-GOB-18. (C, top) Immunoblot analysis of the periplasmic fractions analyzed in panel B with anti-GroEL and anti-DnaK. (Bottom) SDS-PAGE profiles (left) and corresponding immunoblot analysis using anti-GroEL and anti-DnaK (right) of whole-cell extracts of p-preGOB-containing *E. coli* wt and Δ*dacD* cells. Each lane contains the equivalent to 30 μg of total cell proteins. The final positions of the molecular mass markers in the gels are indicated in all cases. For details see Materials and Methods.

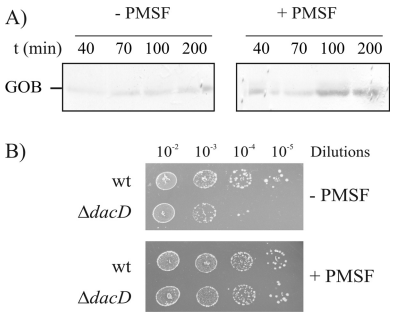

FIG 3 Subinhibitory growth concentrations of the protease inhibitor PMSF increase both periplasmic contents of GOB-18 and concomitant CTX resistance in *E. coli* Δ*dacD* mutants. (A) Time course accumulation of GOB-18 in periplasmic fractions of p-preGOB-containing *E. coli* Δ*dacD* mutants grown in the absence (−PMSF) or presence of 0.12 mM PMSF (+PMSF) in the culture medium. For details see the legend to Fig. 2. (B) CTX resistance phenotypes of p-preGOB-containing *E. coli* Δ*dacD* mutants and isogenic wt cells grown in the absence (−PMSF) or presence of 0.12 mM (+PMSF). For details see the legend to Fig. 1.

protein secretion or increased cell lysis resulting from the Δ*dacD* mutation, was responsible for the reduced GOB-18 contents.

The bacterial periplasm is rich in proteases, and proteins that fail to rapidly acquire the stable native conformation are promptly removed from this compartment, a situation that also applies to GOB-18 variants containing point mutations that reduce protein stability (6, 10, 30). The results shown above thus prompted us to evaluate whether secreted GOB-18 forms were more susceptible to protease attack in Δ*dacD* mutants. In this context, supplementation of culture media with subinhibitory growth concentrations of the serine protease inhibitor phenylmethylsulfonyl fluoride (PMSF) has been found to increase the yields of slowly folding recombinant proteins directed to the *E. coli* periplasm (30). By taking advantage of this observation, we analyzed whether the secreted apo forms of GOB-18 in *E. coli* Δ*dacD* mutants were more accessible to protease attack (Fig. 3). As seen in the figure, a higher accumulation of GOB-18 was observed in periplasmic fractions of Δ*dacD* mutants grown in the presence of PMSF, while no significant increments were seen in wt cells under similar conditions (Fig. 3A and data not shown). In agreement, PMSF addition to the culture media also restored GOB-mediated CTX resistance in Δ*dacD* mutants to levels observed in wt bacteria (Fig. 3B).

The above observations indicated an increased accessibility of secreted GOB-18 forms to periplasmic proteases in cells lacking DacD and reinforce the notion that this LMM PBP plays roles in the final steps of biogenesis of this MBL.

Loss of DacD increases biofilm formation in *E. coli* and *S. enterica*. LMM PBPs are generally believed to play roles in the remodeling of PG and the modulation of bacterial morphology (17, 31). However, a variety of studies have indicated that some LMM PBPs endowed with DD-carboxypeptidase activity may also have roles in other processes such as biofilm formation (17, 31). In fact, in *E. coli* strains, mutations deleting LMM PBP4, -5, or -7 affected biofilm formation and combinations of deletions had cumulative effects (17, 31, 32). Also, treatment of *E. coli* with subinhibitory concentrations of different β-lactam antibiotics alters the ability of the cells to form biofilms, with some β-lactam groups increasing biofilm growth and others inhibiting it (32), thus suggesting that the inhibition of different PBPs may have differential (and even opposite) effects on the ability of *E. coli* cells to form biofilms.

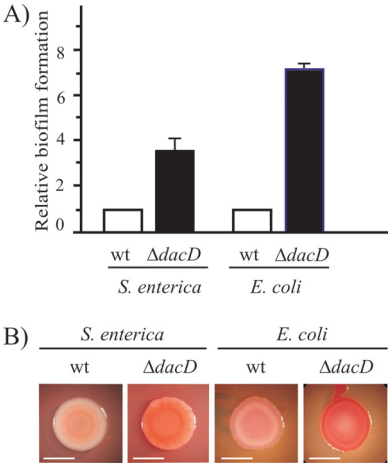

FIG 4 Biofilm growth in Δ*dacD* mutants of *S. enterica* and *E. coli*. (A) Polystyrene cell adhesion. Δ*dacD* mutants of *S. enterica* 1344 or *E. coli* BW25113 (Δ*dacD*) and the corresponding isogenic wt cells (wt), in all cases lacking plasmid p-preGOB, were grown for 48 h at 30°C in 0.15 ml liquid LB in 96-well polystyrene plates, and cell attachment was evaluated by crystal violet staining. The averages and standard deviations from triplicate assays are shown. (B) Colony morphotypes of the above strains on Congo red plates. Bars, 5 mm. For details see Materials and Methods.

Biofilm growth is a complex process that requires the proper secretion and assembly of different macromolecules such as those responsible for motility and adhesion (33–36). Given the potential roles of DacD in the biogenesis of secreted GOB-18 shown above, we decided to evaluate next whether this LMM PBP could also have functions in biofilm growth (Fig. 4). As seen in the figure, Δ*dacD* mutants of *S. enterica* and *E. coli* both showed increased polystyrene attachment abilities, reaching values 3.6- and 7.1-fold higher, respectively, than those of the corresponding wt strains. In agreement, both Δ*dacD* mutants also showed increased Congo red binding morphotypes (Fig. 4B), indicating altered production of surface curli and exopolysaccharide adhesins (33–36). To our knowledge these represent the first bacterial phenotypes described for bacterial mutants lacking DacD.

DISCUSSION

We studied in this and in previous (5, 10, 11) works the pathway(s) leading to the productive biogenesis of MBLs in Gram-negative bacteria, using as a model the expression of the *Elizabethkingia meningoseptica* GOB-18 MBL gene in *E. coli* and *S. enterica*. Secretion of pre-apo GOB-18 is driven by the Sec machinery, implying that final folding and Zn^{2+} assembly to acquire the native MBL form occur in the periplasm (5). Proteins emerging into the periplasm from the Sec channel are greeted by an environment that has a different substance bioavailability and is much more crowded than the cytoplasm and in which the semipermeable peptidoglycan (PG) layer, a myriad of PG-synthesizing and -remodeling enzymes, and large envelope protein complexes are situated (6–8, 17, 18, 34, 35). Individual folding/assembly landscapes of secreted macromolecules are certainly affected in this complex and highly dynamic scenario, and it is therefore not surprising to find a number of periplasmic proteins with the ability to assist the folding, assembly, transit, and degradation of secreted proteins (6–8, 26, 27). Yet, whether the final biogenesis steps of MBLs also require assistance by periplasmic factors represented an open question, although evidence from a number of experiments (9, 11, 12) pointed in this direction. The results presented here indicate that the final steps of GOB-18 MBL biogenesis can be significantly affected by periplasmic factors. We found that mutational losses of the *dacD* gene in *S. enterica* and *E. coli* were concomitant with significant reductions of GOB-18-mediated CTX resistance. The reductions in CTX resistance observed in Δ*dacD* mutants of both species were associated with reduced accumulation of GOB-18 in the periplasm. Since neither the global patterns of secreted proteins nor the OM barrier functions were significantly altered in the Δ*dacD* mutants, the overall observations suggested more-specific roles for DacD in the final biogenesis steps of GOB-18. In agreement with this hypothesis, we found that secreted GOB-18 forms were more rapidly degraded by periplasmic proteases in the Δ*dacD* mutants.

DacD is a periplasmic LMM PBP endowed with low DD-carboxypeptidase activity that is ubiquitously distributed among Gram-negative bacterial species, but a well-defined function has still not be identified (15–20). LMM PBPs displaying DD-carboxypeptidase activity are generally thought to be modulators of bacterial morphology and, in fact, mutational losses of the LMM PBP5 (DacA) in *E. coli* can result in morphological alterations (15–20). DacD displays around 48% sequence identity with DacA, but it contains larger amounts of β-sheets and lower DD-carboxypeptidase activity (15–20). Moreover, unlike loss of DacA, mutational loss of *E. coli* DacD resulted in no apparent phenotypic consequences, thus suggesting different physiological roles for these LMM PBPs (15–20). In this context, different experimental results suggest roles for the LMM PBP DD-carboxypeptidases in processes other than morphology maintenance such as manipulations of PG structure to modulate biofilm growth and even host immune responses (15–20). The observations reported in this work indicating that mutational losses of DacD resulted in an increased ability of *S. enterica* and *E. coli* cells to develop biofilm growth are in line with these proposals and also provide evidence for DacD roles in the PG remodeling machinery.

Several explanations, not necessarily mutually exclusive, could thus account for the observations presented in this work. In principle, DacD could exert a protective "holding" role against protease attack typical of many chaperones (8) to recently secreted apo GOB-18 forms that have not yet acquired a stable conformation capable of Zn^{2+} assembly to reach the native structure. The anchorage of DacD to the periplasmic side of the inner membrane (15, 17, 18) and thus in close proximity to the SecYEG tunnel exit could in fact facilitate such a chaperone-like role.

An alternate possibility is that the loss of DacD affects indirectly the final steps of GOB-18 biogenesis due to its roles in PG remodeling. In fact, disturbances of the highly concerted PG remodeling machinery, albeit rarely lethal, are still reflected in an altered production of secreted macromolecules such as those participating in motility and adhesion (17, 18, 34–36). The overall observations reported here reinforce the notion of more-active roles than previously envisaged for the LMM PBPs in the biogenesis of secreted macromolecules, such as the provision of adequate scaffold functions for macromolecular assembly or the temporal or spatial provision of particular substrates or degradation products derived from PG metabolism (17, 34, 35). Further studies will certainly clarify the exact role(s) of DacD in the final biogenesis steps of GOB-18 in the bacterial periplasm.

ACKNOWLEDGMENTS

We are indebted to T. J. Silhavy for his generous gift of anti-OmpA antisera. We are grateful to A. Vila (IBR-CONICET) for suggestions and critically reading of the manuscript.

This work was supported by grants from CONICET and Agencia Nacional de Promoción Científica y Técnica (Argentina) to A.M.V. J.M.-B. and A.M.V. are career investigators of CONICET, and L.B. a former Fellow of this institution.

REFERENCES

1. **Bonomo RA, Rossolini GM.** 2008. Importance of antibiotic resistance and resistance mechanisms. Expert Rev. Anti Infect. Ther. **6:**549–550. http://dx.doi.org/10.1586/14787210.6.5.549.
2. **Frere JM, Galleni M, Bush K, Dideberg O.** 2005. Is it necessary to change the classification of beta-lactamases? J. Antimicrob. Chemother. **55:**1051–1053. http://dx.doi.org/10.1093/jac/dki155.
3. **Hall BG, Salipante SJ, Barlow M.** 2003. The metallo-beta-lactamases fall into two distinct phylogenetic groups. J. Mol. Evol. **57:**249–254. http://dx.doi.org/10.1007/s00239-003-2471-0.
4. **Crowder MW, Spencer J, Vila AJ.** 2006. Metallo-beta-lactamases: novel weaponry for antibiotic resistance in bacteria. Acc. Chem. Res. **39:**721–728. http://dx.doi.org/10.1021/ar0400241.
5. **Moran-Barrio J, Limansky AS, Viale AM.** 2009. Secretion of GOB metallo-beta-lactamase in Escherichia coli depends strictly on the cooperation between the cytoplasmic DnaK chaperone system and the Sec machinery: completion of folding and Zn(II) ion acquisition occur in the bacterial periplasm. Antimicrob. Agents Chemother. **53:**2908–2917. http://dx.doi.org/10.1128/AAC.01637-08.
6. **Duguay AR, Silhavy TJ.** 2004. Quality control in the bacterial periplasm. Biochim. Biophys. Acta **1694:**121–134. http://dx.doi.org/10.1016/j.bbamcr.2004.04.012.
7. **Silhavy TJ, Kahne D, Walker S.** 2010. The bacterial cell envelope. Cold Spring Harb. Perspect. Biol. **2:**aoo414. http://dx.doi.org/10.1101/cshperspect.a000414.
8. **Gershenson A, Gierasch LM.** 2011. Protein folding in the cell: challenges and progress. Curr. Opin. Struct. Biol. **21:**32–41. http://dx.doi.org/10.1016/j.sbi.2010.11.001.
9. **Wommer S, Rival S, Heinz U, Galleni M, Frere JM, Franceschini N, Amicosante G, Rasmussen B, Bauer R, Adolph HW.** 2002. Substrate-activated zinc binding of metallo-beta-lactamases: physiological importance of mononuclear enzymes. J. Biol. Chem. **277:**24142–24147. http://dx.doi.org/10.1074/jbc.M202467200.
10. **Moran-Barrio J, Lisa MN, Vila AJ.** 2012. In vivo impact of Met221 substitution in GOB metallo-beta-lactamase. Antimicrob. Agents Chemother. **56:**1769–1773. http://dx.doi.org/10.1128/AAC.05418-11.
11. **Moran-Barrio J, Gonzalez JM, Lisa MN, Costello AL, Peraro MD, Carloni P, Bennett B, Tierney DL, Limansky AS, Viale AM, Vila AJ.** 2007. The metallo-beta-lactamase GOB Is a mono-Zn(II) enzyme with a novel active site. J. Biol. Chem. **282:**18286–18293. http://dx.doi.org/10.1074/jbc.M700467200.
12. **Hu Z, Gunasekera TS, Spadafora L, Bennett B, Crowder MW.** 2008. Metal content of metallo-beta-lactamase L1 is determined by the bioavailability of metal ions. Biochemistry **47:**7947–7953. http://dx.doi.org/10.1021/bi8004768.
13. **Alami N, Hallenbeck PC.** 1995. Cloning and characterization of a gene cluster, phsBCDEF, necessary for the production of hydrogen sulfide from thiosulfate by Salmonella typhimurium. Gene **156:**53–57. http://dx.doi.org/10.1016/0378-1119(94)00930-Q.
14. **Heinzinger NK, Fujimoto SY, Clark MA, Moreno MS, Barrett EL.** 1995. Sequence analysis of the phs operon in Salmonella typhimurium and the contribution of thiosulfate reduction to anaerobic energy metabolism. J. Bacteriol. **177:**2813–2820.
15. **Baquero MR, Bouzon M, Quintela JC, Ayala JA, Moreno F.** 1996. dacD, an Escherichia coli gene encoding a novel penicillin-binding protein (PBP6b) with DD-carboxypeptidase activity. J. Bacteriol. **178:**7106–7111.
16. **Nelson DE, Young KD.** 2001. Contributions of PBP 5 and DD-carboxypeptidase penicillin binding proteins to maintenance of cell shape in Escherichia coli. J. Bacteriol. **183:**3055–3064. http://dx.doi.org/10.1128/JB.183.10.3055-3064.2001.
17. **Ghosh AS, Chowdhury C, Nelson DE.** 2008. Physiological functions of D-alanine carboxypeptidases in Escherichia coli. Trends Microbiol. **16:**309–317. http://dx.doi.org/10.1016/j.tim.2008.04.006.
18. **Vollmer W, Bertsche U.** 2008. Murein (peptidoglycan) structure, architecture and biosynthesis in Escherichia coli. Biochim. Biophys. Acta **1778:**1714–1734. http://dx.doi.org/10.1016/j.bbamem.2007.06.007.
19. **Sarkar SK, Dutta M, Chowdhury C, Kumar A, Ghosh AS.** 2011. PBP5, PBP6 and DacD play different roles in intrinsic beta-lactam resistance of Escherichia coli. Microbiology **157:**2702–2707. http://dx.doi.org/10.1099/mic.0.046227-0.
20. **Chowdhury C, Kar D, Dutta M, Kumar A, Ghosh AS.** 2012. Moderate deacylation efficiency of DacD explains its ability to partially restore beta-lactam resistance in Escherichia coli PBP5 mutant. FEMS Microbiol. Lett. **337:**73–80. http://dx.doi.org/10.1111/1574-6968.12009.
21. **Baba T, Ara T, Hasegawa M, Takai Y, Okumura Y, Baba M, Datsenko KA, Tomita M, Wanner BL, Mori H.** 2006. Construction of Escherichia coli K-12 in-frame, single-gene knockout mutants: the Keio collection. Mol. Syst. Biol. **2:**2006.0008. http://dx.doi.org/10.1038/msb4100050.
22. **Hughes KT, Roth JR.** 1988. Transitory cis complementation: a method for providing transposition functions to defective transposons. Genetics **119:**9–12.
23. **Datsenko KA, Wanner BL.** 2000. One-step inactivation of chromosomal genes in Escherichia coli K-12 using PCR products. Proc. Natl. Acad. Sci. U. S. A. **97:**6640–6645. http://dx.doi.org/10.1073/pnas.120163297.
24. **Guzman LM, Belin D, Carson MJ, Beckwith J.** 1995. Tight regulation, modulation, and high-level expression by vectors containing the arabinose PBAD promoter. J. Bacteriol. **177:**4121–4130.
25. **Harrison JS, Keshavarz-Moore E, Dunnill P, Berry MJ, Fellinger A, Frenken L.** 1997. Factors affecting the fermentative production of a lysozyme-binding antibody fragment in Escherichia coli. Biotechnol. Bioeng. **53:**611–622. http://dx.doi.org/10.1002/(SICI)1097-0290(19970320)53:6<611::AID-BIT9>3.0.CO;2-P.
26. **Rouviere PE, Gross CA.** 1996. SurA, a periplasmic protein with peptidyl-prolyl isomerase activity, participates in the assembly of outer membrane porins. Genes Dev. **10:**3170–3182. http://dx.doi.org/10.1101/gad.10.24.3170.
27. **Dartigalongue C, Raina S.** 1998. A new heat-shock gene, ppiD, encodes a peptidyl-prolyl isomerase required for folding of outer membrane proteins in Escherichia coli. EMBO J. **17:**3968–3980. http://dx.doi.org/10.1093/emboj/17.14.3968.
28. **Hoiseth SK, Stocker BA.** 1981. Aromatic-dependent Salmonella typhimurium are non-virulent and effective as live vaccines. Nature **291:**238–239. http://dx.doi.org/10.1038/291238a0.
29. **Zhang XS, Garcia-Contreras R, Wood TK.** 2007. YcfR (BhsA) influences Escherichia coli biofilm formation through stress response and surface hydrophobicity. J. Bacteriol. **189:**3051–3062. http://dx.doi.org/10.1128/JB.01832-06.
30. **Anba J, Bernadac A, Lazdunski C, Pages JM.** 1988. Improving the stability of a foreign protein in the periplasmic space of Escherichia coli. Biochimie **70:**727–733. http://dx.doi.org/10.1016/0300-9084(88)90101-0.
31. **Gallant CV, Daniels C, Leung JM, Ghosh AS, Young KD, Kotra LP, Burrows LL.** 2005. Common beta-lactamases inhibit bacterial biofilm formation. Mol. Microbiol. **58:**1012–1024. http://dx.doi.org/10.1111/j.1365-2958.2005.04892.x.
32. **Boehm A, Steiner S, Zaehringer F, Casanova A, Hamburger F, Ritz D, Keck W, Ackermann M, Schirmer T, Jenal U.** 2009. Second messenger signalling governs Escherichia coli biofilm induction upon ribosomal stress. Mol. Microbiol. **72:**1500–1516. http://dx.doi.org/10.1111/j.1365-2958.2009.06739.x.
33. **Romling U.** 2005. Characterization of the rdar morphotype, a multicellular behaviour in Enterobacteriaceae. Cell. Mol. Life Sci. **62:**1234–1246. http://dx.doi.org/10.1007/s00018-005-4557-x.
34. **Scheurwater EM, Burrows LL.** 2011. Maintaining network security: how macromolecular structures cross the peptidoglycan layer. FEMS Microbiol. Lett. **318:**1–9. http://dx.doi.org/10.1111/j.1574-6968.2011.02228.x.
35. **Koraimann G.** 2003. Lytic transglycosylases in macromolecular transport systems of Gram-negative bacteria. Cell. Mol. Life Sci. **60:**2371–2388. http://dx.doi.org/10.1007/s00018-003-3056-1.
36. **Monteiro C, Fang X, Ahmad I, Gomelsky M, Romling U.** 2011. Regulation of biofilm components in Salmonella enterica serovar Typhimurium by lytic transglycosylases involved in cell wall turnover. J. Bacteriol. **193:**6443–6451. http://dx.doi.org/10.1128/JB.00425-11.
37. **Sambrook J, Fritsch EF, Maniatis T.** 1989. Molecular cloning: a laboratory manual, 2nd ed. Cold Spring Harbor Laboratory Press, Cold Spring Harbor, NY.